Science Advances
AAAS

advances.sciencemag.org/cgi/content/full/6/36/eaba3992/DC1

Supplementary Materials for

Primary cilium-dependent cAMP/PKA signaling at the centrosome regulates neuronal migration

Julie Stoufflet, Maxime Chaulet, Mohamed Doulazmi, Coralie Fouquet, Caroline Dubacq, Christine Métin, Sylvie Schneider-Maunoury, Alain Trembleau, Pierre Vincent*, Isabelle Caillé*

*Corresponding author. Email: isabelle.caille@upmc.fr (I.C.); pierre.vincent@upmc.fr (P.V.)

Published 2 September 2020, *Sci. Adv.* **6**, eaba3992 (2020)
DOI: 10.1126/sciadv.aba3992

The PDF file includes:

Other Supplementary Material for this manuscript includes the following:

(available at advances.sciencemag.org/cgi/content/full/6/36/eaba3992/DC1)

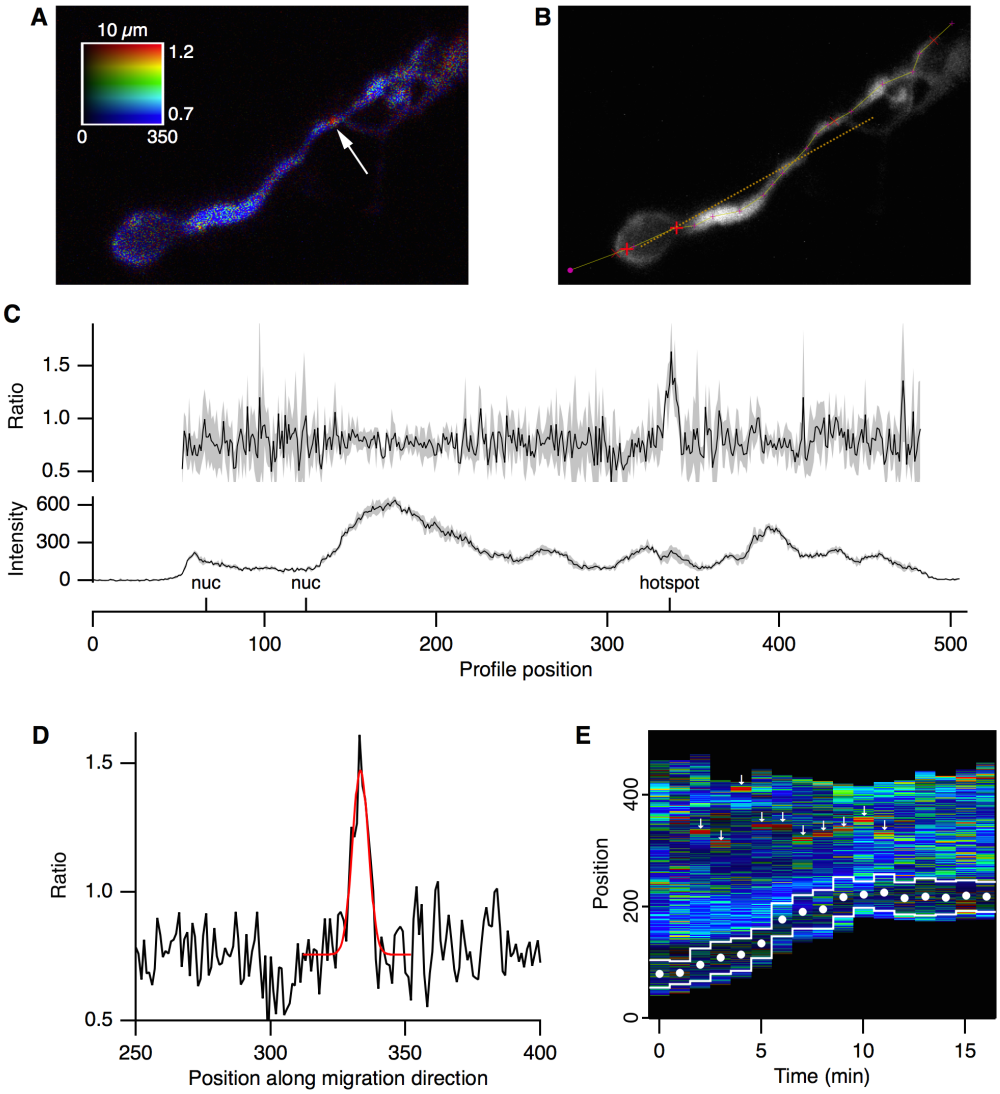

Figure S1. **Analysis of cAMP hotspot on ratio images.**
A) Ratio image: the hotspot is indicated by the arrow.
B) Intensity image (acceptor fluorescence). A series of anchor points (purple "+") were manually positioned along the length of the cell.
C) Ratio and intensity profiles calculated along these line segments, over a width of 4 pixels. Gray shading indicates standard deviation. The intensity profile was annotated manually for every time-point of the recording, marking both sides of the nucleus (red X on B, and "nuc" on C). The trajectory of the nucleus center during the migration was fitted to a line (yellow dotted line on B).
D) Profile measurements were then resampled in the coordinates defined by this trajectory. The profile ratio at the hotspot was fitted to a Gaussian function (red curve). The width of the hotspot was estimated as 2x the width parameter of the gaussian fit, i.e. the width of the red curve at 1/e height.
E) Kymograph representation of ratio profiles. The nucleus border is indicated with the white lines, the center by (•) and hotspots by small arrows. The large arrow indicates the time-point illustrated in A-D. Pixel size: 0.113 µm.

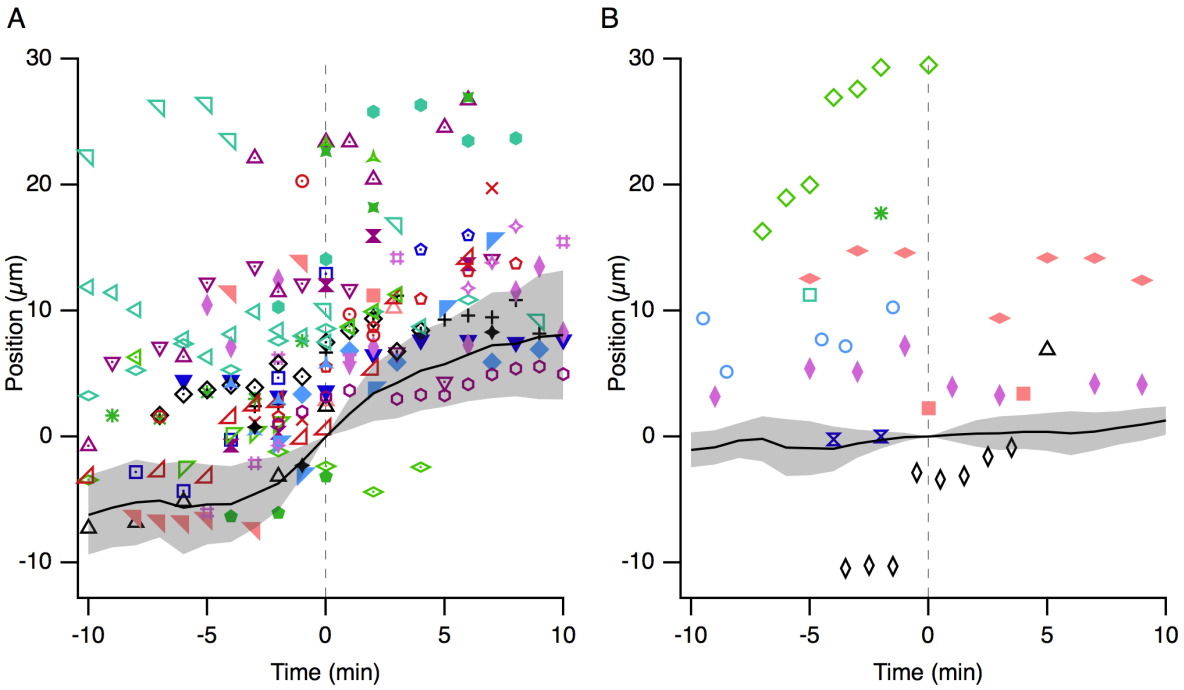

Figure S2: **Spatio-temporal distribution of hotspots in migrating and non-migrating neurons.**

A) Profiles of 44 migrating neurons (also displayed as a heatmap in Fig. 2A) are superimposed in the same coordinate system as that used for kymographs (Fig. 1D, E). Time 0 is defined as the midpoint of NK. Position 0 corresponds to the position of the nucleus center at t=0. The black line with sigmoid shape shows the average trajectories of nucleus centers, reflecting NK movement. Gray shading indicates standard deviation. All hotspots in this series of experiments are presented by a symbol, with a same color and marker for a same experiment. Most hotspots appear ahead of the nucleus, while a few can appear next to or behind the nucleus (see for example Fig. 2C).

B) Same representation as A) for 20 neurons which showed no NK (also displayed as a heatmap in Fig. 2B and in kymograph Fig. 1F). Time 0 is defined as the midpoint of the recording. Note that among these 20 neurons, only nine display a hotspot represented here.

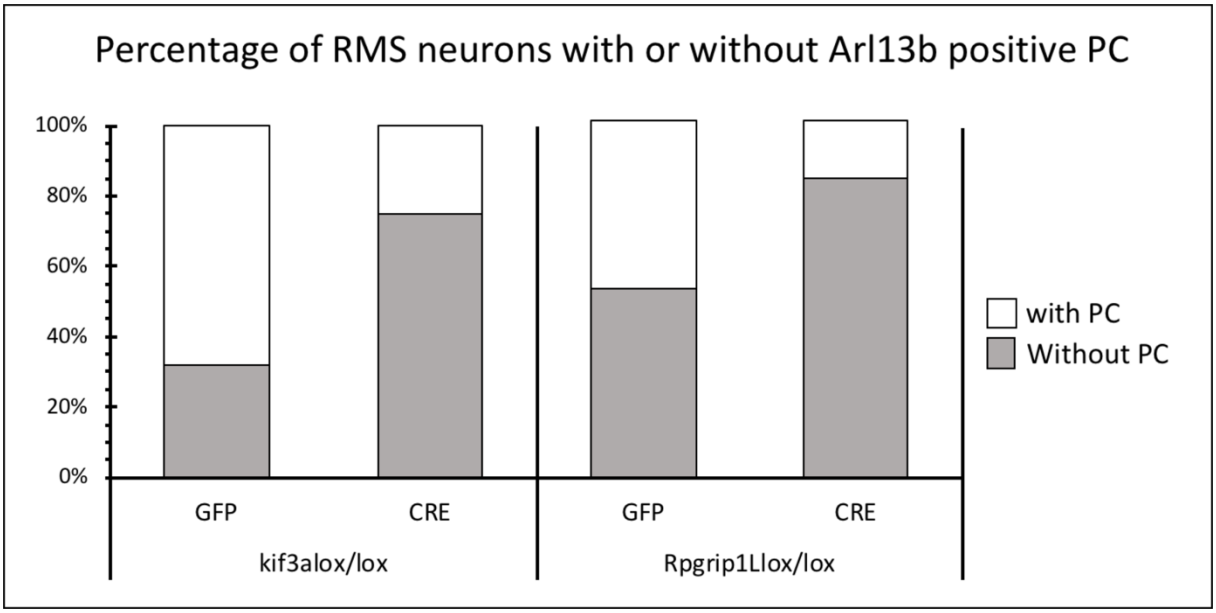

Figure S3 **Efficiency of cilium ablation after Cre electroporation in Kif3a$^{lox/lox}$ and Rpgrip1l$^{lox/lox}$ mice:**
The percentage of GFP-positive neurons displaying a γ-tubulin positive centrosome associated with an Arl13B positive PC was significantly reduced in Cre-injected Kif3a$^{lox/lox}$ mice (*34*) (25% in CRE (n=14, N=3) versus 68,3% in GFP (n=109, N=3), $p<0.001$) and Rpgrip1l$^{lox/lox}$ mice (*35*) (16.2% in CRE (n=99, N=3) versus 47% in GFP (n=68, N=3), Chi-squared test $p<0.001$).

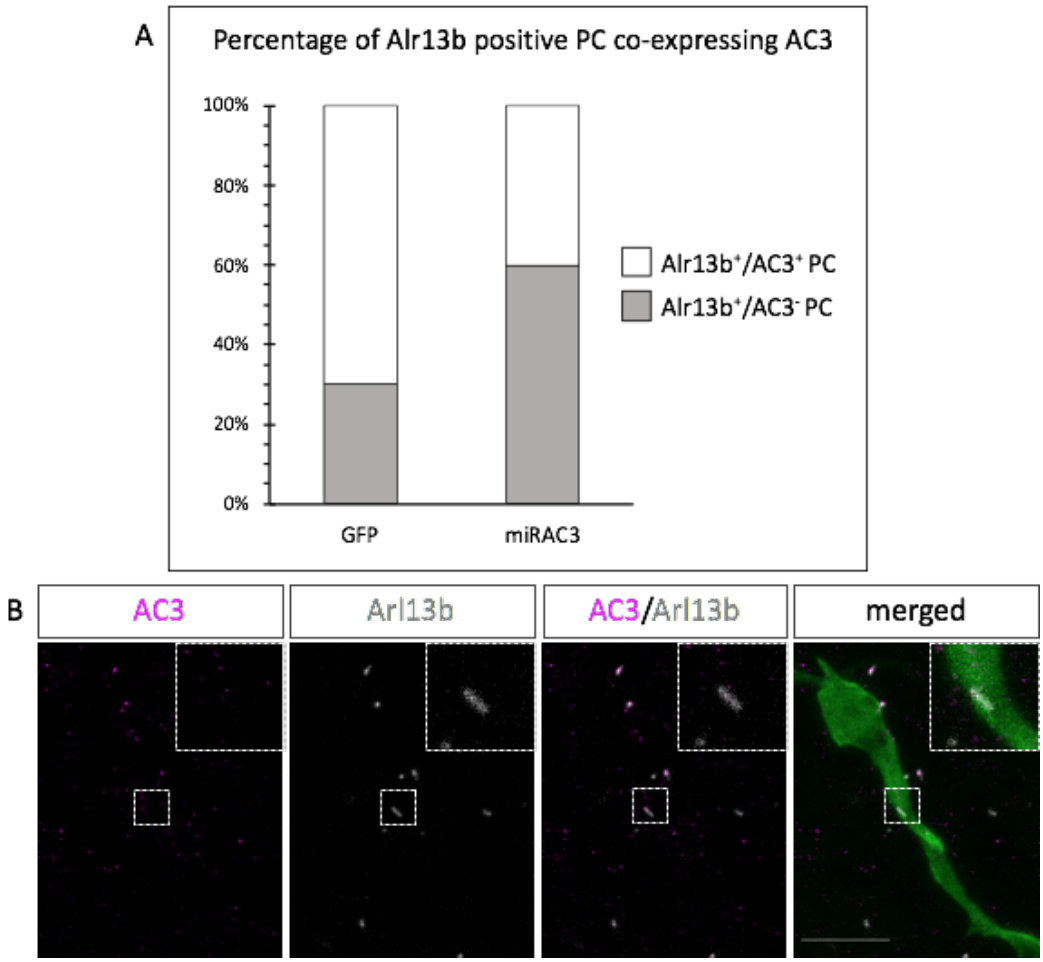

Figure S4: **Efficiency of MirAC3 knock-down**

A) The percentage of GFP neurons displaying an Arl13B and AC3 immunoreactive PC was significantly reduced in miRAC3 transfected neurons (70% in GFP (N=3, n=47) versus 40% in mirAC3 (N=3, n=63)). (X-squared=10.066, df=1, $p<0.01$)

B) Immunocytochemistry of a mirAC3-GFP electroporated neuron showing an intact ARL13B immunopositive PC (grey) without AC3 immunoreactivity (magenta). Scale-bar: 10µm

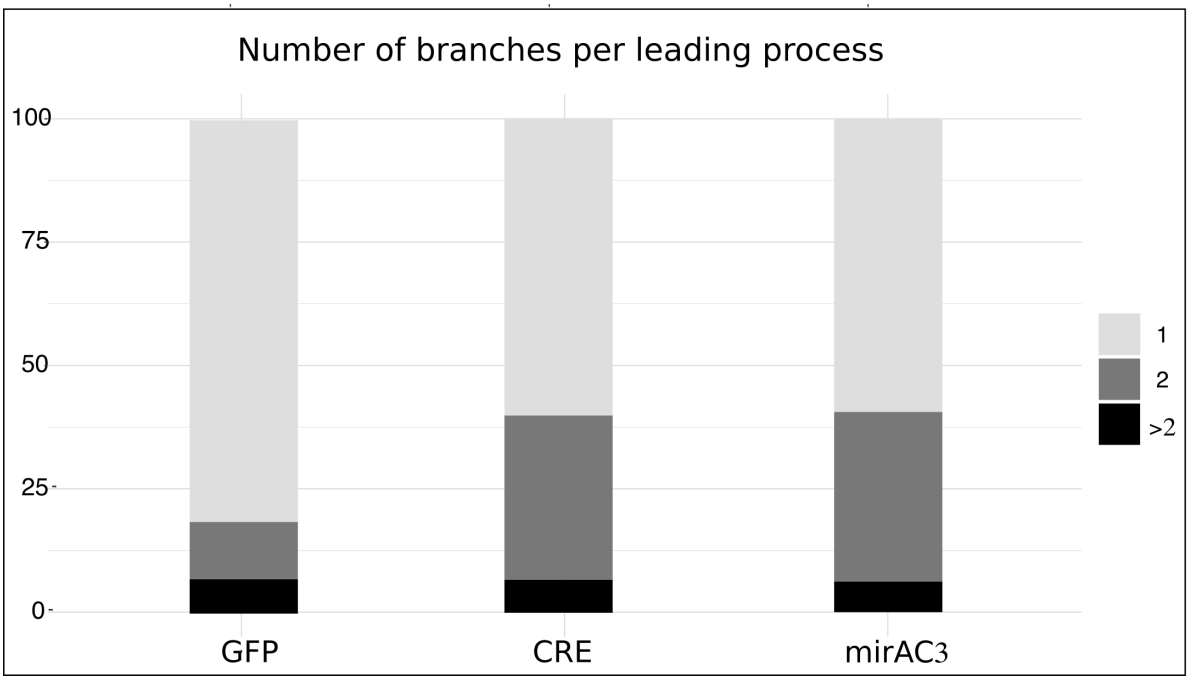

Figure S5: **PC-ablation and AC3 KD affect the morphology of the leading process**
GFP: 87,5% of cells with 1 branch, 12,5% with 2 branches and 0% with more than 2. CRE: 60% of cells with 1 branch, 33,33% with 2 branches and 6,67% with more than 2 branches. mirAC3; 57,6% of the cells with 1 branch, 33,33% with 2 branches and 9,09% with more than 2 branches (Fisher exact test, p-value = 0.01649) GFP: N=3, n=40, CRE: N=3, n=30, mirAC3: N=3, n=33)

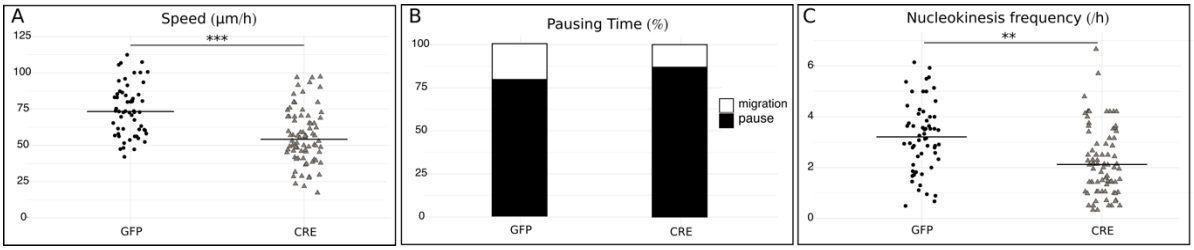

Figure S6: **Migration defects after primary cilium ablation in Rpgrip1l$^{lox/lox}$ mice**

A) Speed of neurons electroporated with GFP or CRE-GFP in Rpgrip1l$^{lox/lox}$ background: the speed was slowed-down in cilium-ablated neurons (GFP 75.33±2.45 µm/h versus CRE 57.88±2.43 µm/h, $p<0.001$, student-test $t(136) = 4.86$, $p<0.001$)

B) Percentage of pausing time of neurons electroporated with GFP or CRE-GFP in Rpgrip1L background: the pausing time was increased in cilium-ablated neurons (GFP 77% versus CRE 85% , $p<0.001$, Pearson's Chi-squared test $X^2= 48.66$, p-value < 0.001)

C) Nuclear translocation frequency of neurons electroporated with GFP or CRE-GFP in Rpgrip1l background: the frequency of NK was reduced in cilium-ablated neurons (GFP 3.23± 0.18 NK/h versus CRE 2.26± 0.15 NK/h, $p=0.03$, Mann-Whitney test $U (136) =3.01$, $p= 0.03$)

The black lines represent the median. GFP: N=4, n=58, CRE: N=3, n=80

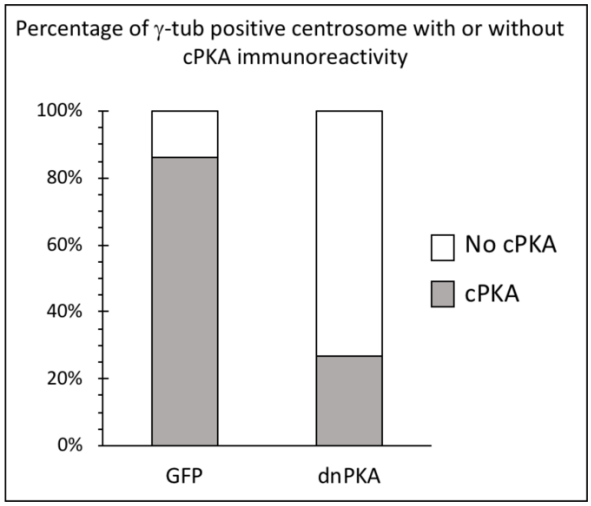

Figure S7: **efficiency of PKA delocalization by dnPKA**

dnPKA efficiently delocalized PKA from the centrosome (26.67% of neurons with visible cPKA immunoreactivity at the centrosome in dnPKA (n=30 N=2) versus 86.05% in GFP (n=44 N=3) (X-squared = 26.352, df=1, $p<0.001$).

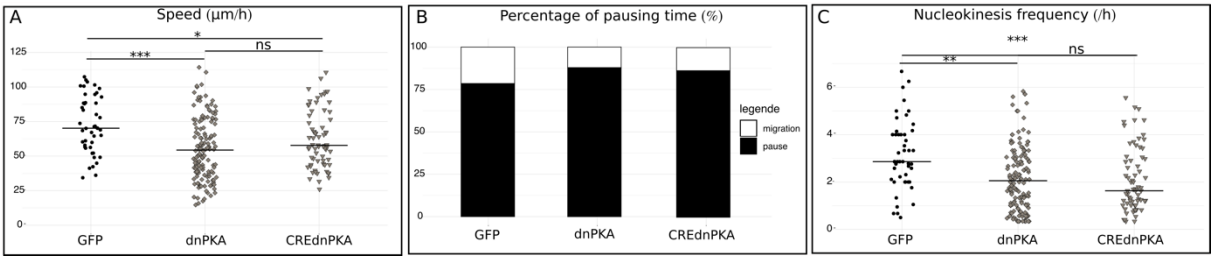

Figure S8: **Migration defects after PKA delocalization alone or PKA delocalization along with cilium ablation.**

The CREdnPKA neurons are not significantly different from the dnPKA neurons for the three parameteres analyzed

A) Speed of neurons electroporated with GFP, dnPKA-GFP or dnPKA-GFP plus CRE-TdTomato in Kif3a$^{lox/lox}$ background: GFP 75.49±3.48 µm/h versus dnPKA 55.76±1.90 µm/h and CREdnPKA 63.73±2.85 µm/h (one-way anova($F_{(4,383)}$=7.87, p<0.001, followed by Tukey HSD test (* p<0.05, *** p<0.001)

B) Percentage of pausing time of neurons electroporated with GFP, dnPKA-GFP or dnPKA-GFP/CRE-TdTomato in Kif3a$^{lox/lox}$ background: 76% in GFP versus dnPKA 86% and CREdnPKA 84% (Pearson's Chi-squared test X^2= 67.25, p<0.001)

C) Nuclear translocation frequency of neurons electroporated with GFP, dnPKA-GFP or dnPKA-GFP/CRE-TdTomato in Kif3a$^{lox/lox}$ background: GFP 3.15±0.21 NK/h versus dnPKA 2.23±0.12 NK/h and CREdnPKA 2.09±0.16 NK/h (One-way Kruskal-Wallis test (Chi square X^2= 19.57, p<0.001, df=4, followed by Nemenyi test (* p<0.05, *** p<0.001)

The black line represents the median. GFP: N=3, n=48, dnPKA: N=3, n=146, CREdnPKA: N=3, n=86

Supplementary movies

Movie S1. cAMP biosensor in a control migrating neuron
Movie S2: cAMP biosensor in a control migrating neuron
Movie S3: cAMP biosensor in a control non-migrating neuron
Movie S4. cAMP insensitive biosensor in a control migrating neuron
Movie S5. cAMP biosensor in a kif3a recombined migrating neuron
Movie S6. cAMP biosensor in a Rpgrip1L recombined migrating neuron
Movie S7. cAMP biosensor in an AC3 knocked-down migrating neuron
Movie S8: cAMP biosensor in a control migrating neuron transiently displaying two hotspots
Movie S9. GFP migrating neurons (control condition)
Movie S10. Cre-GFP migrating neurons (kif3a recombined condition)
Movie S11. MirAC3-GFP migrating neurons (AC3 KD condition)
Movie S12. GFP + CentrinRFP migrating neuron (control condition)
Movie S13. Cre-GFP + CentrinRFP migrating neuron (kif3a recombined condition)
Movie S14. dnPKA-GFP + tdTomato migrating neurons (delocalized PKA condition)
Movie S15. dnPKA-GFP + CRE-tdTomato migrating neurons (delocalized PKA + kif3a recombined condition)
Movie S16. cAMP biosensor in a radially migrating neuron of the postnatal olfactory bulb
Movie S17. cAMP biosensor in a tangentially migrating neuron of the adult RMS
Movie S18. cAMP biosensor in a radially migrating neuron of the embryonic cortex (E19)